WM'07 Conference, February 25 – March 1, 2007, Tucson, AZ

The Effect of Waste Loading on The Structure and Leach Resistance of Borosilicate Glass for Savannah River Site Sb2 Waste Immobilization

S.V. Stefanovsky
SIA Radon, 7th Rostovskii lane, Moscow 119121
Russia

J.C. Marra
SRNL, Building 773-42A, Savannah River Site, Aiken, SC 29808
USA

ABSTRACT

A High Level Waste (HLW) surrogate with chemical composition corresponding to the Savannah River Site Sludge Batch 2 (SB2) composition was vitrified using a commercially available lithium-sodium-borosilicate frit 320 in a laboratory resistive furnace and inductive cold crucible melter (ICCM). The waste loading in these tests ranged between 45 and 65 wt.%. The vitrified products were composed of a major vitreous matrix and a minor crystalline phase with the magnetite-type spinel structure. The content of the spinel phase in the products increased from 3-6 vol.% at 45 wt.% waste loading to 18-20 vol.% at 60 wt.% waste loading due to an increase of iron oxide content in the glasses. Moreover, traces of sulfate/chloride-bearing "yellow" phase were observed on the surface of glass with 55 wt.% waste loading melted in the resistive furnace at a temperature of 1200 ^{0}C whereas no "yellow" phase was found in the product produced in the cold crucible. The "yellow" phase was present in the products with 60 wt.% waste loading melted in the resistive furnace at temperatures of 1200 and 1250 ^{0}C but its content significantly decreased after melting at 1300 ^{0}C and it disappeared after melting at 1350 ^{0}C due to thermal decomposition of sodium sulfate. The product with the same waste loading but melted in the cold crucible did not contain the "yellow" phase. Uranium in all the products entered the vitreous phase and variation in waste loading resulted in a minor effect on uranium speciation. Leachability data determined using the Product Consistency Test (PCT) procedure demonstrated similar normalized release and leach rate values of B, Li, Na, and Si for the products with 45 to 50 wt.% waste loading. At waste loadings equal to or greater than about 55 wt % there was an apparent decrease in durability. This is likely due to destruction of the glass network and formation of a nepheline phase in the glass.

INTRODUCTION

In our previous work [1-3] we described the results of cold crucible tests on vitrification of HLW surrogate with the Savannah River Site Sludge Batch 2 (SB2) composition using a commercially available lithium-sodium-borosilicate frit 320. Very high specific glass productivity (up to ~118 kg/(m^{2}h) and stable operation of the cold crucible have been demonstrated. The glasses were

composed of a vitreous matrix and contained ~10-15 vol.% magnetite-type spinel phase. The glasses exhibited low values of Li, Na, B and Si release which were found to be 15 to 30 times lower than the reference Environmental Assessment (EA) glass used for waste form repository acceptance. Uranium at 45 wt.% waste loading enters the vitreous phase and occurs predominantly in a hexavalent form (~80% of total U) [4]. In the present work we investigate the effect of waste loading on the degree of crystallinity of the materials and uranium speciation in more detail. Results obtained for the glassy materials produced in a laboratory resistive furnace and in the cold crucible were compared.

EXPERIMENTAL

Chemical composition of the Savannah River Site Sludge Batch 2 (SB2) waste and target chemical compositions of frit 320 and glasses are given in Table I and II. Waste loading content ranged between 45 and 65 wt.%. Batches were prepared according to SRT-ITB-2004-00027 procedure [5] including precipitation of MnO_2 and Fe, Ni and sodium-uranyl hydroxides (in the cold crucible tests uranium was not introduced) from nitrate solutions.

In the lab-scale tests mixtures of reagent-grade chemicals were placed in 100 ml alumina crucibles which were heated in a resistive furnace to temperatures ranging between 1150 ^{0}C and 1350 ^{0}C (depending on waste loading in glass) and kept at this temperature for 1 h. A portion of the glass melt from each composition was poured onto a metal plate and the remainder was cooled to room temperature in a furnace overnight (furnace turned off).

Table I. Concentration of Anion/Cation Content of Sludge SB2 Feed Simulants (air dried at 115° C).

Cations	Content, wt.%	Anions	Content, wt.%
Al^{3+}	6.27	CO_3^{2-}	3.59
Ba^{2+}	0.17	F^-	0.01
Ca^{2+}	1.89	Cl^-	1.06
Cr^{3+}	0.18	I^-	0.03
Cu^{2+}	0.11	NO_2^-	4.10
Fe^{3+}	20.81	NO_3^-	1.70
K^+	0.05	OH^-	33.10
Mg^{2+}	0.10	O^{2-}	4.10
Mn^{4+}	2.12	PO_4^{3-}	0.13
Na^+	6.31	SO_4^{2-}	0.70
Ni^{2+}	1.20	**Properties**	
Pb^{2+}	0.21	Specific gravity. g/cm^3	~1.15
Si^{4+}	0.65	Total solids. wt.%	~20
Sr^{2+}	0.06		
U^{6+}*	7.29	Soluble solids. wt.%	~3
Zn^{2+}	0.22	Total organic carbon. wt. %	
Zr^{4+}	0.41		<0.05

* cold crucible tests were U-free.

Table II. Chemical composition (wt.%) of frit 320 and glassy products (target and measured values).

Oxides	Waste	Frit 320	SB2-45		SB2-50		SB2-55		SB2-60		SB2-65	
			T	V	T	V	T	V	T	V	T	V
Li_2O	-	8.00	4.40	nd	4.00	nd	3.60	nd	3.20	nd	2.80	nd
B_2O_3	-	8.00	4.40	nd	4.00	nd	3.60	nd	3.20	nd	2.80	nd
F	0.01	-	0.01	nd	0.01	nd	0.01	nd	0.01	nd	0.01	nd
Na_2O	12.08	12.00	12.04	11.86	12.04	12.00	12.04	11.53	12.05	13.61	12.05	14.11
MgO	0.24	-	0.11	0.47	0.12	0.84	0.13	0.87	0.14	0.88	0.15	0.94
Al_2O_3	16.83	-	7.57	7.42	8.41	7.62	9.26	8.68	10.10	9.75	10.94	12.07
SiO_2	1.98	72.00	40.47	41.56	37.01	38.25	33.47	35.80	30.00	33.34	26.48	32.65
P_2O_5	0.14	-	0.06	0.31	0.07	0.56	0.08	0.53	0.08	0.54	0.09	0.41
SO_3	0.83	-	0.37	0.41	0.41	0.36	0.46	0.24	0.50	0.32	0.54	0.30
Cl	1.51	-	0.68	0.27	0.75	0.38	0.83	0.38	0.90	0.37	0.98	0.34
K_2O	0.09	-	0.04	0.12	0.04	0.10	0.05	0.11	0.05	0.11	0.06	0.12
CaO	3.76	-	1.69	1.66	1.88	1.88	2.07	2.16	2.25	2.78	2.44	3.01
TiO_2	-	-	-	0.07	-	0.04	-	0.12	-	0.12	-	0.12
Cr_2O_3	0.37	-	0.17	0.13	0.19	0.06	0.21	0.13	0.22	0.14	0.24	0.06
MnO	3.89	-	1.75	1.47	1.94	1.47	2.14	1.67	2.33	1.34	2.53	1.24
Fe_2O_3	42.26	-	19.02	16.91	21.14	18.26	23.24	20.04	25.36	15.28	27.46	12.61
NiO	2.17	-	0.98	0.43	1.08	0.23	1.19	0.21	1.30	0.18	1.41	0.10
CuO	0.20	-	0.09	0.15	0.10	0.18	0.11	0.18	0.12	0.30	0.13	0.17
ZnO	0.39	-	0.18	0.22	0.19	0.12	0.21	0.28	0.23	0.25	0.25	0.12
SrO	0.10	-	0.05	1.32	0.05	3.03	0.06	2.91	0.06	2.83	0.07	2.33
ZrO_2	0.79	-	0.35	0.38	0.39	0.42	0.43	0.23	0.47	0.56	0.51	0.13
I	0.04	-	0.02	-	0.02	-	0.02	-	0.03	-	0.03	-
BaO	0.27	-	0.12	0.22	0.13	0.19	0.15	0.20	0.16	0.29	0.18	0.34
PbO	0.32	-	0.14	0.21	0.16	0.07	0.18	0.17	0.19	0.19	0.21	0.24
U_3O_8	11.75	-	5.29	5.22	5.87	5.89	6.46	6.55	7.05	7.35	7.64	8.61
Total	100.0	100.0	100.0	90.82	100.0	91.93	100.0	92.99	100.0	90.54	100.0	90.02
WL, wt.%			45		50		55		60		65	

T – target composition, V – vitreous phase composition, WL – waste loading, nd – not determined.

The cold crucible tests were performed in the Radon bench-scale (~216 mm in diameter) and full-scale (~418 mm in diameter) vitrification units. Equipment and tests procedures were described in detail in ref. [1-3].

Chemical compositions of the glassy products were determined using X-ray fluorescence (XRF) spectroscopy using a PW-2400 Philips Analytical BV unit equipped with quantitative analytical Philips SuperQuantitative & IQ-2001 Software, atomic absorption spectroscopy (AAS) using a

Perkin-Elmer 403 spectrometer, and emission flame photometry (EFP) to determine Na and K using a PFM-U 4.2 flame photometer (Russian design). The glassy materials were characterized with X-ray diffraction (XRD) using a DRON-4 diffractometer, scanning electron microscopy with energy dispersive system (SEM/EDS) using a JSM-5300 + Link ISIS analytical unit, and infrared (IR) spectroscopy using an IKS-29 spectrophotometer with compaction of powdered glass in KBr pellets. Uranium speciation in the products was investigated by X-ray absorption spectroscopy (XANES/EXAFS) using a Kurchatov Institute synchrotron beam line. Leach resistance of glasses was determined using the PCT procedure (7-day crushed glass leach test at 90 ^{0}C) [6].

RESULTS

Lab-scale tests

To obtain uniform products, it was necessary to increase the temperature of glass melting from 1150 ^{0}C at 45 wt.% waste loading to 1400 ^{0}C at 65 wt.% waste loading. For example, for the material with 60 wt.% waste loading, the melts obtained at 1200 and 1250 °C were very viscous and hard to pour from the crucible, while solidified samples from the crushed crucibles contained the yellow phase (Figure 1, upper row) . At 1300 °C, the melt viscosity was lower, but we were still not able to pour it from the crucible completely, and a melt sample from the crushed crucible contained some traces of the yellow phase (Figure 1, middle row). The melt produced at 1350 °C remained viscous, but it could be poured from the crucible. No yellow phase was observed, probably, due to decomposition of sodium sulfate and volatilization of sodium chloride (Figure 1, lower row).

XRD patterns of the glassy products with 45 to 65 wt.% waste loading are shown in Figure 2. At low waste loading (45 wt.%) glass is the predominant phase in the product whereas crystalline phase content is low (~4 vol.%). The only phase found in the lab-glasses at any waste loadings is spinel. The major peak due to the spinel phase is split (Figure 2). As follows from SEM examination, two different spinel phases occur. One of them is enriched with NiO and, in some extent, ZnO; another one is enriched with iron (Table III). Chemical composition of the latter is close to magnetite.

Increasing of waste loading results in higher degree of crystallinity in the materials (Figures 2 and 3) with a maximum of ~23 vol.% in the material with 65 wt.% waste loading. SEM images show that the spinel phase occurs as regular individual or aggregated grains (Figure 3). At high waste loadings, secondary devitrification of the vitreous phase yields crystallization of a “star-like” spinel phase with different chemical composition (Figure 3, *6*). As expected, the spinel phases concentrate iron and transition metals (iron group elements) and serves as a host phase for corrosion products of HLW (Table III). The vitreous phase accumulates alkali and alkali earth elements as well as uranium (Table I). The vitreous phase is strongly depleted with iron group elements.

Fig. 1. Vitrified samples produced in a lab-scale resistive furnace at various temperatures

Infra-red spectra of the materials prepared in a resistive furnace within the wavenumber range of 1600-400 cm^{-1} (Figure 4) consist of four broad bands located at 1500-1300 cm^{-1}, 1200-850 cm^{-1}, 800-700 cm^{-1} and 600-400 cm^{-1}. The first of the above-listed bands centered about 1400 cm^{-1} is attributed to either deformation vibrations in water molecules or valence vibration in CO_3^{2-} ions which are often present on the surface of powdered glasses [7]. The broad band at 1200-850 cm^{-1} with maximum at ~1000 cm^{-1} is due to overlapping of the bands of valence vibrations of bridging Si-O-Si and non-bridging $Si-O^-$ bonds in the silicon-oxygen glass network [7,8]. Increase of waste loading in the glassy material results in some increase in intensity and narrowing of this band with a shift of its maxima towards lower wavenumbers. This is likely due to an increase in the number of broken bonds in the glass network at the lower silica concentration and an increase of network-modifier content in the glass (Table II). This is also consistent with behavior of the band 800-700 cm^{-1}. Major contribution to this band is due to symmetric ν_s valence vibrations of bridging Si-O-Si bonds. With the increase of waste loading in the glass this band decreases in its intensity. The broad band at 600-400 cm^{-1} is mainly due to deformation vibrations in the silicon-oxygen groups, but appreciable contribution to this band may be caused by tetrahedral [FeO_4] groups in both the vitreous phase and in the spinel [9]. It is

likely that valence vibrations in spinel are responsible for appearance and intensity increase of the band with a maximum at ~560 cm^{-1} (Figure 4).

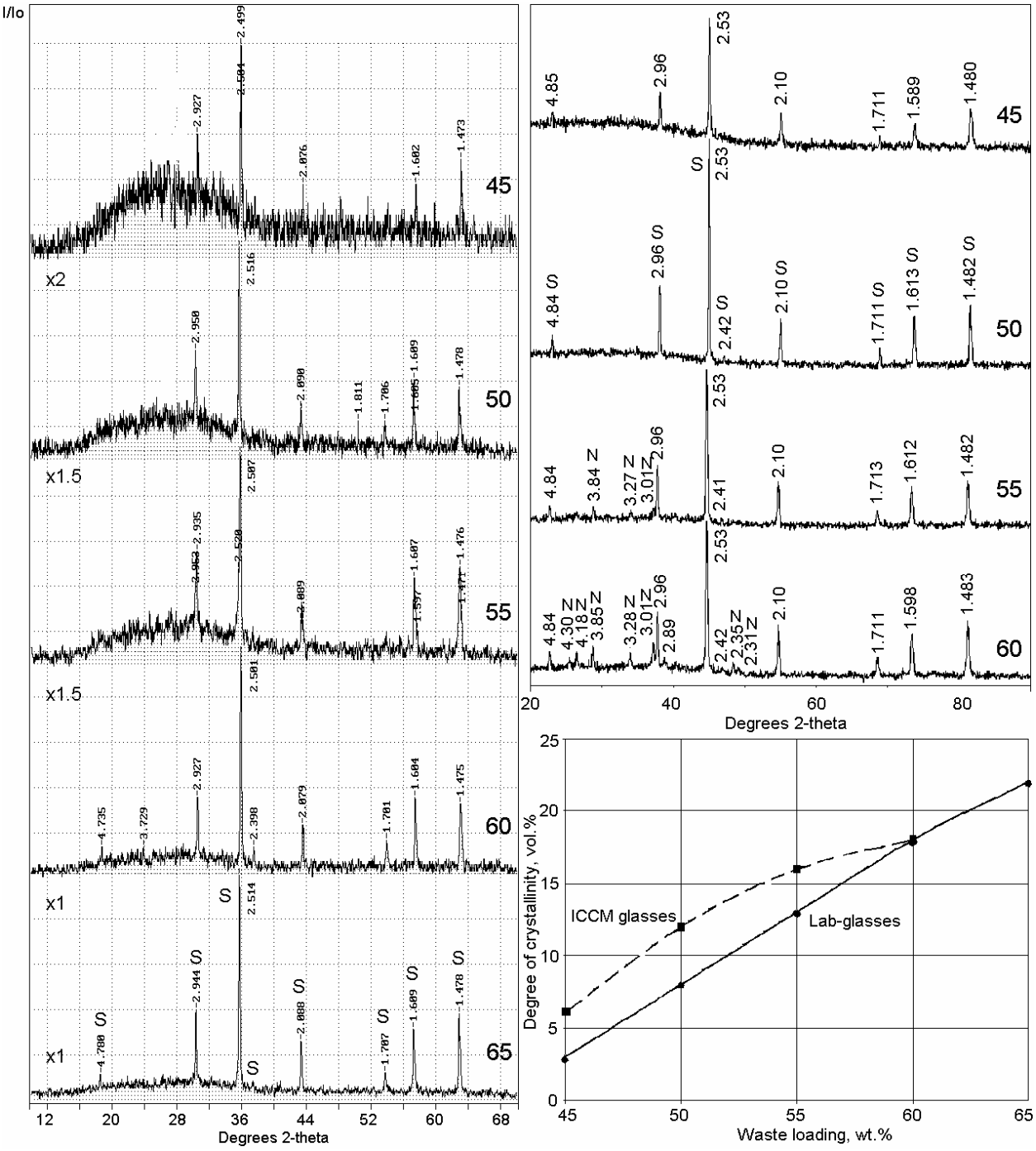

Figure 2. XRD patterns of the glassy materials produced in lab-scale resistive furnace (left) and cold crucibles (upper right) and the degree of crystallinity of materials vs waste loading.

Table III. Chemical compositions of spinel structure phases.

	SB2-45		SB2-50	SB2-55			SB2-60	SB2-65
Oxides	45-1.	45-2.	50	55-1	55-2	55-3	60	65
Al_2O_3	0.83	-	1.04	1.35	1.60	1.49	2.30	3.16
Cr_2O_3	0.61	-	1.01	1.00	11.92	0.88	1.69	1.38
MnO	4.62	4.85	5.51	5.71	6.37	5.97	5.32	5.66
Fe_2O_3	74.62	86.14	77.57	75.79	68.33	80.29	75.8	75.81
NiO	17.14	4.22	13.71	12.13	9.62	7.55	11.92	10.23
ZnO	0.15	-	-	0.74	1.05	0.81	-	0.78
Total	97.97	95.21	98.84	96.72	98.89	96.99	97.03	97.02
Ions	Formula units							
Al^{3+}	0.04	-	0.05	0.06	0.07	0.07	0.10	0.14
Cr^{3+}	0.02	-	0.03	0.03	0.35	0.03	0.05	0.04
Mn^{2+}	0.15	0.16	0.18	0.19	0.20	0.19	0.17	0.18
Fe^{3+}	2.15	2.48	2.20	2.19	1.90	2.28	2.16	2.14
Ni^{2+}	0.53	0.13	0.42	0.37	0.29	0.23	0.36	0.31
Zn^{2+}	0.00	-	-	0.02	0.03	0.02	-	0.02
Total	2.89	2.77	2.86	2.86	2.84	2.81	2.84	2.84
O^{2-}	4.00	4.00	4.00	4.00	4.00	4.00	4.00	4.00

IR spectra of UO_3 demonstrate strong absorption at about 900 cm^{-1}, which is assigned to asymmetric ν_3 vibrations in the uranyl UO_2^{2+} ions [7]. The bands at 535 and 475 cm^{-1} are likely due to vibration U-O_{eq} between uranium and equatorial oxygen atoms [10]. The bands at 1400 cm^{-1}, 1615 cm^{-1} as well as strong broad absorption at 3600-3000 cm^{-1} (not shown on Figure 4) may be assigned to deformation and valence vibrations in molecules of absorbed or structurally bonded water. As it is seen from the IR spectra of the U-bearing glasses (Figure 4, left) the bands due to vibrations of the U-O bonds are located in the same range as strong bands due to vibrations of Si-O bonds and their contribution to the bands 1150-850 cm^{-1} and 600-400 cm^{-1} is insignificant because of relatively low uranium content in the glassy materials as compared with silicon and iron oxide contents.

X-ray absorption spectra of U L_{III} edge in UO_3 and UO_2 and the glasses prepared in the resistive furnace (Figure 4, lower right) are very similar to those presented in ref. [11,12]. No appreciable effect of waste loading and uranium content in the glassy materials on spectral characteristics of uranium was observed. Uranium is predominantly hexavalent. The fraction of tetravalent uranium does not exceed 15-20%. This is in a good agreement with reference data [12,13] and our previous XPS data [4].

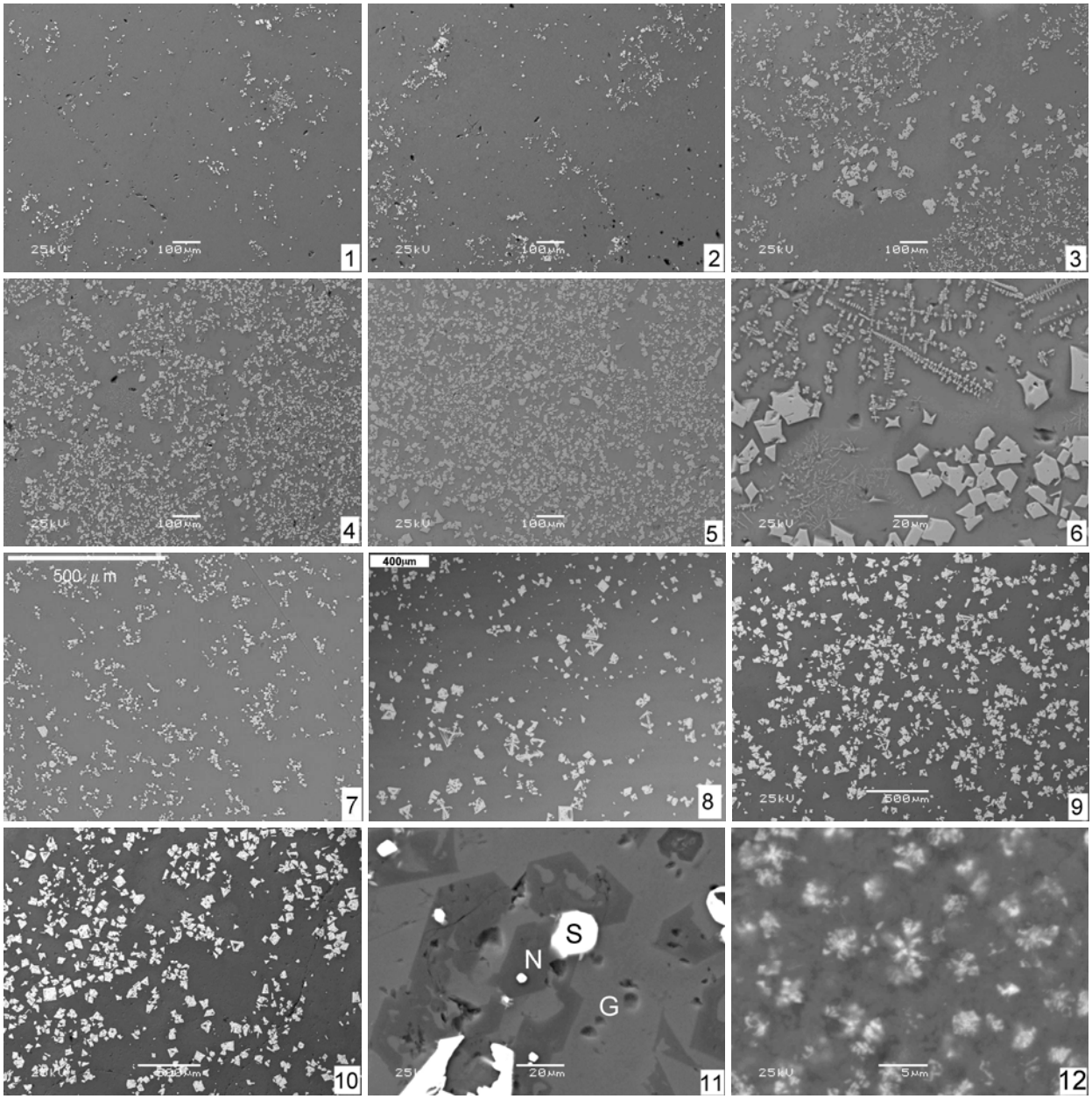

Figure 3. SEM images of the glassy materials prepared in lab-scale resistive furnace (1-6) and cold crucibles (7-12).

Waste loading, wt.%: 1,7 – 45; 2,8 – 50; 3,9 – 55; 4,10-12 – 60; 5,6 – 65.
G – glass, N – nepheline, S – spinel.

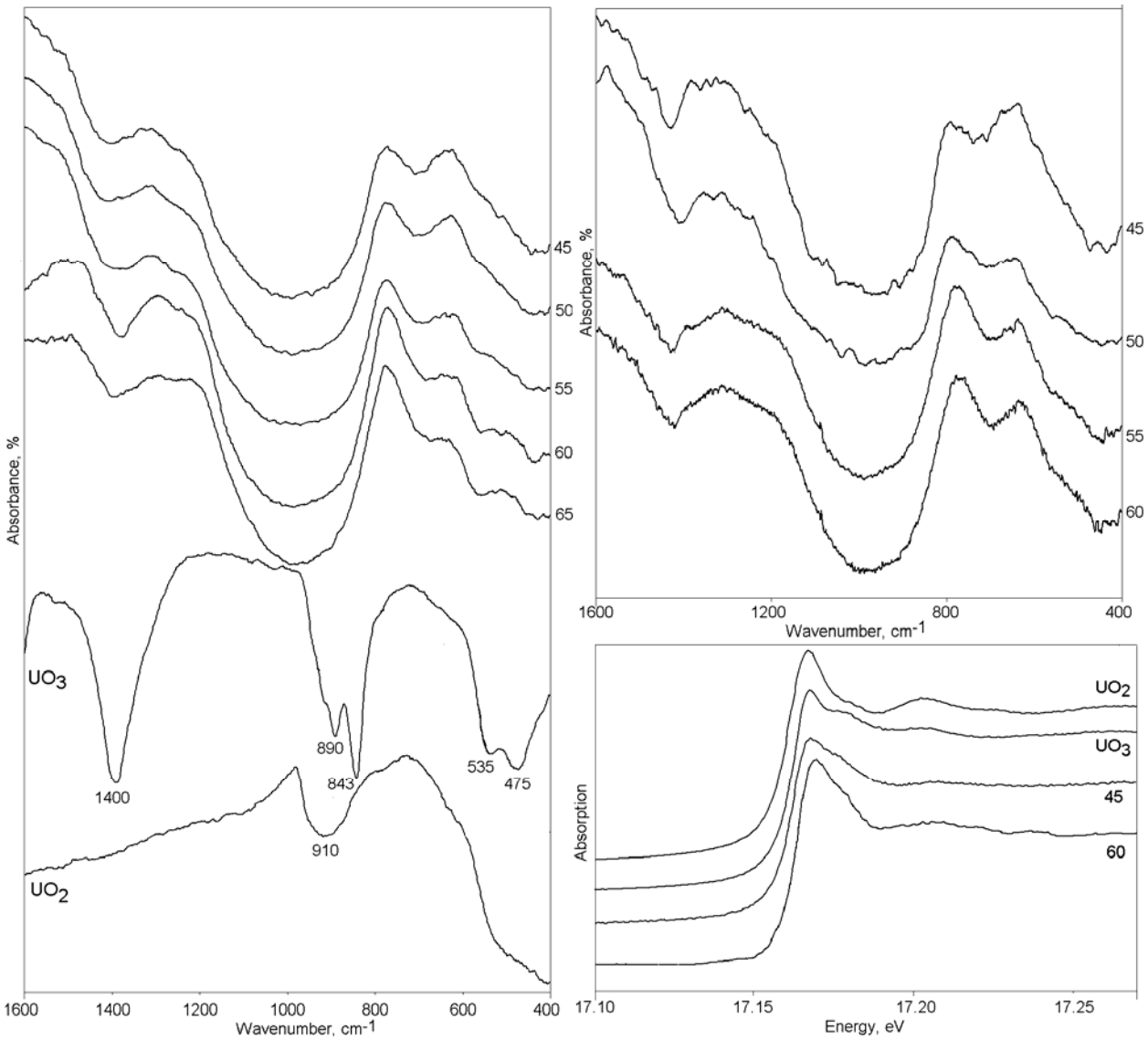

Figure 4. Infra-red spectra of uranium oxides and lab-scale prepared (left) and cold crucible produced (upper right) glassy materials, and X-ray absorption spectra of uranium oxides and U-bearing lab-scale prepared glassy materials.

Cold crucible tests

The phase composition and structure of glassy materials produced in the cold crucible testing are somewhat different from those prepared in alumina crucibles in the lab-scale resistive furnace. The differences are due to different thermal history of the materials. Melts produced in cold crucibles were poured into 10 L carbon steel containers and annealed in a tunnel furnace. As a result, the cooling rate of these glasses was much lower than that of lab-scale furnace.

Actual bulk chemical composition of the glassy materials and chemical compositions of co-existing vitreous and crystalline phases are given in Table IV. The materials produced in cold crucibles have some higher degree of crystallinity (Figure 2) and did not contain "yellow phase".

Table IV. Bulk chemical composition of the glassy materials produced in cold crucibles by XRF analysis and chemical composition of co-existing phases (wt.%) by EDS data.

Components	45 wt.% waste loading			50 wt.% waste loading			~55 wt.% waste loading				60 wt.% waste loading			
	Bulk	Glass	Spinel	Bulk	Glass	Spinel	Bulk	Glass	Spin.1	Spin.2	Bulk	Glass	Spinel	Neph.
B_2O_3	4.20	nd	-	4.00	nd	-	2.25	nd	-	-	2.60	nd	-	
Na_2O	12.14	12.52	0.48	12.29	13.26	0.21	13.19	15.27	-	-	12.98	14.35	-	14.24
MgO	0.17	0.12	0.23	0.00	0.14	0.12	0.22	0.75	2.44	2.34	0.20	0.59	1.70	1.15
Al_2O_3	8.30	8.21	1.24	11.49	12.41	1.66	12.42	13.25	2.97	2.54	12.17	12.78	2.18	21.33
SiO_2	41.38	43.03	0.97	43.48	49.22	1.48	30.58	33.66	-	-	31.05	33.42	-	40.07
P_2O_5	0.03	0.34	<0.01	0.31	0.59	-	0.14	0.31	-	-	0.15	0.32	-	-
SO_3	0.11	0.62	0.08	0.00	0.22	-	0.24	0.18	-	-	0.31	0.21	-	-
Cl	0.18	0.00	<0.01	0.00	0.24	-	0.08		-	-	0.09		-	-
K_2O	0.13	0.15	0.02	0.20	0.16	-	0.13	0.13	-	-	0.14	0.17	-	0.35
CaO	1.82	2.02	0.08	2.59	2.99	-	3.17	3.47	-	-	3.16	3.44	-	-
TiO_2	0.05	nd	nd	0.00	nd	nd	0.02	nd	nd	nd	0.02	nd	nd	nd
Cr_2O_3	0.29	0.09	0.36	0.06	0.10	0.95	0.17	0.01	2.58	1.09	0.13	0.04	1.73	-
MnO	1.83	1.33	4.33	2.01	1.79	4.34	2.54	1.32	4.56	5.04	2.42	1.19	5.91	-
Fe_2O_3	22.31	21.28	80.24	21.57	14.10	81.76	32.28	14.76	75.34	80.18	31.66	16.42	81.99	6.25
NiO	0.73	0.16	12.43	0.51	0.11	8.88	0.92	0.08	8.45	9.16	0.79	0.03	6.60	-
CuO	0.14	0.20	0.06	0.08	0.28	nd	0.22	0.17	1.64	1.38	0.22	0.14	1.42	-
ZnO	0.23	0.00	0.20	0.38	0.10	nd	0.20	0.18	1.71	1.62	0.19	0.16	0.57	-
SrO	0.05	1.82	0.07	1.16	1.81	-	0.66	0.79	-	-	0.61	1.33	-	1.76
ZrO_2	0.41	0.37	<0.01	0.18	0.39	-	0.58	0.54	-	-	0.54	0.23	-	-
BaO	0.19	0.13	<0.01	0.45	0.16	-	0.25	0.30	-	-	0.25	0.27	-	-
PbO	0.14	0.15	0.24	0.58	0.50	-	0.23	0.26	-	-	0.16	0.14	-	-
Total	94.83	92.52	101.00	97.35	98.57	99.40	100.49	85.43	99.69	103.35	99.84	85.23	102.60	85.15

Note: Li_2O was not determined, nd – not determined by EDS.

At high waste loading (60 wt.%) secondary devitrification of the vitreous phase and formation of a nepheline phase occurred (Figure 2, upper right and Figure 3, *11,12*). The increase in the degree of crystallization is due to the much lower cooling rate of the glassy materials in both the containers and "dead volume" of the cold crucible. Two types of spinel structure phases with slightly different iron oxide contents were found. One of them forms cubic individual and aggregated crystals and appear to be segregated from the glass melt at early stages of solidification. The second variety forms star-like crystals at later stage of solidification being a product of secondary devitrification of the matrix vitreous phase. Nepheline was segregated at the latest stage of devitrification at the lowest cooling rates. Quenched melts did not contain the nepheline phase. Major constituents of this phase are sodium, aluminum and silicon oxides but some iron and minor strontium and magnesium are also present substituting for aluminum and sodium and/or potassium, respectively.

Infra-red spectra of the cold crucible melted materials are very similar to those of lab-scale prepared materials (Figure 4). These spectra show numerous absorption bands exhibiting formation of both spinel (wavenumber range lower 800 cm^{-1}) and aluminosilicate (nepheline) type phases (1200-850 cm^{-1}) or at least crystallites or nanocrystals preceding crystal formation.

Study of chemical durability of the materials produced in the cold crucibles using PCT-A procedure (Table V) demonstrates low values of normalized release of major glass constituents. At waste loadings of 45-50 wt.% normalized release values remain low – even lower than those of the glasses with 35 and 40 wt.% waste loading produced in a Joule heated ceramic melter [14] and much lower than the values typical of the EA glass[15]. Increasing of waste loading to ~55 wt.% and higher results in increase of normalized release rate values for all the matrix elements. Two reasons for this effect may be considered. The first one is low silicon and boron oxide contents that causes destruction of the silicon(boron)-oxygen glass network. This is consistent with IR spectroscopic data exhibiting an increase in the number of non-bridging $Si\text{-}O^-$ bonds. The second one is formation of the nepheline phase with low chemical durability.

Table V. Comparative chemical durability of the glassy materials produced in cold crucibles at various waste loadings by PCT-A procedure.

Materials and waste loading, wt.%	Normalized release, g/L			
	B*	Li**	Na*	Si
F320-10/2 (45 %)[1]	0.56	0.49	0.80	0.35
F320-5/3 (50 %)[1]	0.46	0.65	0.74	0.30
F320-10/3 (50 %)[2]	0.64	0.74	0.82	0.35
F320-3/4 (~55 %)[2]	1.40	1.03	1.09	0.40
F320-7/4(60 %)[2]	2.20	1.45	1.28	0.49
F320 (35 %) [14]	1.33	1.25	1.39	0.79
F320 (40 %) [14]	1.47	1.31	1.60	0.79
EA glass [15]	16.70	9.56	13.35	3.92

[1] 216 mm in diameter cold crucible; [2] 418 mm in diameter cold crucible.

Normalized Release Calculation Notes:

* B and Na elemental concentrations in the glass obtained from XFS data.

** Li elemental concentrations in the glass estimated using theoretical concentration for 60 wt % loading and adjusting in accordance with lower waste loading expected in canisters 3 and 5.

DISCUSSION

Comparison of the U-bearing glassy materials prepared in lab-scale resistive furnace and the U-free materials produced in bench- (216 mm in diameter) and industrial-scale (418 mm in diameter) cold crucibles has shown that the features of their phase composition and structure are caused by thermal history (much lower cooling rate for the cold crucible melted samples) rather than chemical composition (if uranium oxides were present or not). Both materials with waste loading ranging between 45 wt.% and 60-65 wt.% are composed of major vitreous phase (≥80 vol.%) and spinel structure magnetite-type phase. Individual or aggregated spinel crystals with rather regular shape are segregated at early stage of crystallization and may reach tens of microns in size. At the highest waste loadings (55 to 60 wt.%) in the central parts of glass containers and

"dead volume" of the cold crucible secondary devitrification of the matrix vitreous phase occurred yielding fine (up to 5-10 μm in size) star-like crystals of the spinel phase but with some different chemical composition (iron-enriched). At the lowest cooling rates crystallization of the nepheline-type phase occurred. No nepheline was found in the lab-scale produced glassy materials due to the higher cooling rate of the samples.

In all the samples, the vitreous phase is enriched with alkali and alkali earth elements and silica. Spinel is strongly enriched with iron and iron-group elements (Cr, Mn, Ni) as well as Cu, Zn, and Mg, whereas U, Zr, Pb, B enter only the vitreous phase. Minor nepheline in the sample with 60 wt.% waste loading incorporates major Na, Al and Si, and minor Fe, Sr, Mg, and K. Uranium is present in predominantly hexavalent form (≥80% of total) as uranyl ions that is consistent with reference [12,13] and our previous data [4].

Normalized release values of the matrix elements (B, Li, Na, Si) increase with increasing of waste loading in the glassy materials. Significant reduction in chemical durability occurs at 55 wt.% or greater waste loading because of destruction of the glass network due to low silica content and crystallization of nepheline phase. Nevertheless the normalized release values remain much lower (by 7-12 times for B, 6-8 times for Li, by 10-12 times for Na, and by 8-10 times for Si) than those in the reference EA glass [15].

CONCLUSION

Comparative examination of the glassy materials produced in laboratory furnace and bench- and industrial-scale cold crucibles have demonstrated possibility of vitrification of SB2 sludges at waste loading of up to ~50-55 wt.%. Such materials are composed of major (>80 vol.%) vitreous phase concentrating alkali, alkali earth elements, silica and uranium and minor (up to ~20 vol.%) spinel structure magnetite type phase enriched with iron and iron group elements as well as Cu, Zn, and Mg. The materials produced in cold crucibles did not contain "yellow phase". They have high chemical durability exceeding chemical durability of the reference EA glass by 10 to 50 times depending on matrix elements considered. Increase of waste loading over ~55 wt.% results in destruction of the glass network and formation of nepheline phase resulting in a reduction in the chemical durability. Uranium exists in a major hexavalent form. No difference in the structure of the U-bearing (up to 7.6-8.6 wt.% U_3O_8) and U-free materials has been found.

ACKNOWLEDGEMENTS

The work was performed under financial support from US DOE on Contract "Advanced Melter Technology Application to the Defense Waste Processing Facility (DWPF) –Cold Crucible Induction Heated Melter (CCIM)". The authors thank SIA Radon personnel who performed the cold crucible vitrification tests, Mr. Boris Nikonov for his help in SEM/EDS study, Nadezhda Penionzkiewic for XRD analyses and Dr. Andrew Shiryaev for XAS spectra record of the samples.

REFERENCES

1. A.P. Kobelev, S.V. Stefanovsky, O.A. Knyasev, T.N. Lashchenova, J.C.Marra, E.W. Holtzscheiter, C.C. Herman, "Induction Heated Cold Crucible Melter Testing with Troublesome High Level Waste Components, " Proc. 107th Amer. Ceram. Soc. Meeting. Baltimore, MD, April 10-13, 2005. P. 159-169.
2. A.P. Kobelev, S.V. Stefanovsky, O.A. Knyazev, T.N. Lashchenova, E.W. Holtzscheiter, J.C. Marra, "Cold Crucible Vitrification of Defense Waste Surrogate and Vitrified Product Characterization," Mat. Res. Soc. Symp. Proc. **932** (2006) 353-360.
3. A.P. Kobelev, S.V. Stefanovsky, O.A. Knyazev, T.N. Lashchenova, A.G. Ptashkin, M.A. Polkanov, E.W. Holtzscheiter, J.C. Marra, "Results of a 50% Waste Loading Vitrification Test Using the Cold Crucible Melter for Savannah River Site," Proc. Waste Management '06 Conf. Tucson, AZ, February 26 – March 2, 2006. CD-ROM. ID 6127. 11p.
4. S.V. Stefanovsky, K.I. Maslakov, A.Y. Teterin, Y.A. Teterin, J.C. Marra, "Uranium Speciation in Borosilicate Waste Glass," Proc. 36iemes Journees des Actinides. Oxford, UK, April 1-4, 2006. P-38.
5. J.C. Marra, E.W. Holtzscheiter, "Sludge and Glass Compositions for Cold Crucible Induction Melter (CCIM) Testing," SRT-ITB-2004-00027, Rev. 0, Savannah River National Laboratory (2004).
6. American Society for Testing and Materials (ASTM). "Standard Test Methods for Determining Chemical Durability of Nuclear, Hazardous, and Mixed Waste Glasses: The Product Consistency Test (PCT)," ASTM C1285-97, West Conshohoken, PA. 1997.
7. K. Nakamoto. "Infrared Spectra of Inorganic and Coordination Compounds," John Wiley & Sons, Inc. New York, London (1964).
8. J. Wong, C.A. Angell, "Glass Science by Spectroscopy," Marcel Dekker, Inc. New York – Basel (1976).
9. I.I. Plusnina, "Infrared Spectra of Minerals," MGU, Moscow (1977).
10. S. Saad, S. Obbade, S. Yagoubi, F. Abraham, Synthesis, Crystal Structure Determination, Infrared and Electrical Characterization of the New Cesium Uranyl Niobate $Cs_9U_8Nb_5O_{41}$," Proc. 36iemes Journees des Actinides. Oxford, UK, April 1-4, 2006. P-35.
11. P.G. Eller, G.D. Jarvinen, J.D. Purson, R.A. Penneman, R.R. Ryan, F.W. Lytle, R.B. Greegor, "Actinide Valences in Borosilicate Glass," Radiochim. Acta. **39** (1985) 17-22.
12. D. Petit-Maire, J. Petiau, G. Calas, N. Jacquet-Francillon, "Local Structure around Actinides in Borosilicate Glasses," Journ. De Physique, Col. C8, Suppl. $n^0$12, **47** (1986) C8-849 – C8-852.
13. B.W. Veal, J.N. Mundy, D.J. Lam, "Actinides in Silicate Glasses," Handbook on the Physics and Chemistry of Actinides," Elsevier Sci. Publ. (1987) 271-310.
14. C.C. Herman, "Summary of Results for Expanded Macrobatch 3 Variability Study," WSRC-TR-2001-00511 (2001).
15. J.R. Harbour, "Summary of Results for Macrobatch 3 Variability Study," WSRC-TR-2000-00351 (2000).